Chemistry Research Journal, 2017, 2(4):84-90

Available online www.chemrj.org

Research Article

ISSN: 2455-8990
CODEN(USA): CRJHA5

Synthesis, structural properties and characterisation of self activating $Na_2Zr(BO_3)_2$

Ş. Gacanoğlu[a]*, H. Güler[a], A. Teke[b], R. Tülek[b]

[a]Balıkesir University, Faculty of Science & Literature, Department of Chemistry, Balıkesir, Turkey
[b]Balıkesir University, Faculty of Science &Literature, Department of Physics, Balıkesir, Turkey

Abstract In this study, the synthesis, characterization and luminescence properties of the self-activated a novels odiumzirkoniumorthoborate ($Na_2Zr(BO_3)_2$) was reported. This compound has been successfully synthesized by solid state reaction at 1000 °C among the initial reactants of Na_2CO_3, ZrO_2 and H_3BO_3 (molar ratio 1: 1: 2). The crystal structure analysis with X-ray powder diffraction showed that the composition crystallized in the orthorhombic system and the composition with the cell parameters of a = 6.7212 Å, b = 11.6591 Å and c = 16.6653 Å, Z = 7, and space group Pmmm (47), The compound in which orthoborate structures are analyzed by FTIR, and a long-luminescent compound by means of PL spectral results.

Keywords Persistent Luminescence, Orthoborate, Alkali metal, Double Metal Borates

Introduction

The industrial use of compounds with permanent luminescence properties are rapidly increasing. In the past studies carried out, compounds which have short luminescence properties need activators such as cations. Permanent and self-luminescent compounds are not frequently encountered. Self reacting persistent luminesence compounds can provide significant advantages in industrial applications in terms of stability, crystal structure alignment, luminescence capacities.

There is a great interest for alkali borate compounds that have magnetic, catalytic and phosphorescent properties [1-2] such as $K_2Zr(BO_3)_2$ [3], $BaZr(BO_3)_2$[4], $CaZr(BO_3)_2$ [5], $SrZr(BO_3)_2$ [6], $PbZr(BO_3)_2$ [7].

Matsuava [8] et al. investigated the luminescence properties of rare earth metal-doped $SrAl_2O_4$ compound. The work carried out rapidly over the following years, but a small number of studies have been carried out on the permanent luminescence properties of borate compounds with a 100% activator concentration, which is a self-activating .

Diaz and Keszler [9] studied the luminescence properties of europium-doped $Ba_2Mg(BO_3)_2$, $Ba_2Ca(BO_3)_2$ and $Sr_2Mg(BO_3)_2$ borate compounds in their work in 1997. There is no study can be found about investigation and identification of the persistant luminescence properties of these alkali borate compounds at time of this paper.

$K_2Zr(BO_3)_2$ synthesized by Akella and Keszler in 1994 structure is identified as persistant luminescent at 2017 by Guifang et al [10].

Guifang et al [10] analyzed the absorption, emission characteristics, permanent and thermoluminescence properties of KZBO and described the band gap of the compound as 5.05 eV. They also described the persistent luminescence property of KZBO originates from the charge transfer in the zirconium complex.

Eechout et al. described numerous non- luminescent compounds that gained luminescence by Eu^{+3} doping [11].

Blasse et al. reported the luminescence in bishmuth borates in 1986. Bi^{+3} ions normally have a low energy absorption band in operation. In a compound of borates, Bi^{+3} ions gains high energy absorption band [12].

Balcerzyk et al reported the luminescence properties of gadolinium borate compounds with added Ce^{+3} and Tb^{+3} and have interpreted the correlation between the increase in dopant ratio and the increase in luminescence property [13]. In our study we report synthesis, characterization and persistent luminescence properties of firstly synthesized sodiumzirconiumborate compound. The luminescence properties, including excitation and emission spectra, luminescence decay is reported. Based on the luminescence properties and thermoluminescence (TL) glow curve the photoluminescence and the persistent luminescence mechanisms are discussed .

2. Experimental

$Na_2Zr(BO_3)_2$ was synthesized by high temperature solid-state reaction of a mixture of high purity Na_2CO_3, ZrO_2 and H_3BO_3 (mol ratios 1:1:2). The mixture was grounded and preheated at 450 °C for 4 hours and the sample was regrounded, annealed and in the following process it was regrounded after being kept at 1000 °C for 24 h. The sample was then cooled to room temperature with 5 °C /minutes. The reaction was carried out by the furnace Protherm PLF 120/10 trademark in the open air. The XRD data were collected using a Panalytical X-Pert Pro diffractometer with the CuK_α radiation (λ: 1.54059Å, 30mA and 40kV), The crystal structure was found and the cell parameters were refined by the POWD program **[14]**. Infrared spectrum was obtained using Perkin Elmer 983G FTIR spectrophotometer in 4000-400 cm^{-1} region with sample as KBr discs.

Temperature dependent photoluminescence measurements were carried out on powders placed in a close-cycled cryostat in the temperature range of 10–300 K and excitation power densities between 0.01 and 1.04 W/cm^2. As an excitation source a frequency tripled Nd:YLFQ-switched pulse laser at 349 nm were used. The luminescence was collected by suitable lenses and then dispersed with a 500 mm spectrometer using 1200 line/mm grating and detected by Intensified Charge Coupled Device (ICCD) camera.

3. Results and Discussion

The basic chemical reaction for the solid-state synthesis of $Na_2Zr(BO_3)_2$ could be suggested by the following chemical equation;

$$Na_2CO_3(k) + ZrO_2(k) + 2H_3BO_3(k) \longrightarrow Na_2Zr(BO_3)_2(k) + CO_2(g) + 3\,H_2O(g) \quad \text{(Eq. A)}$$

The crystal structure of the synthesized compound, $Na_2Zr(BO_3)_2$ was found as orthorombic with the unit cell parameters of a= 6.7212 Å, b=11.6591 Å and c=16.6653 Å, space group Pmmm by driving POWD program**[14].** The density of the $Na_2Zr(BO_3)_2$ was measured by pyknometer using toluene as solvent and found as 3.000 g/cm^3 and Z was calculated as 7. The XRD pattern and data are given in Table.1 and Fig 1.

Table 1: X-ray powder diffraction data of $Na_2Zr(BO_3)_2$

2θ	**hkl**	**I/I_o**	**Orthorombic $Na_2Zr(BO_3)_2$ Space group Pmmm(47)**		
			d_{calc}	**d_{exp}**	**Difference ($x10^{-4}$)**
15.94	003	100	5.5551	5.5557	0.1
20.85	121	18.79	4.2577	4.2616	0.4
22.82	122	34.36	3.8935	3.8962	0.7
28.12	211	7.64	3.1702	3.1663	1.4
29.49	124	11.81	3.0265	3.0279	0.1
31.45	034	6.90	2.8419	2.8423	0.8
32.20	006	1.28	2.7775	2.7766	0.7
33.69	125	69.18	2.6577	2.6581	0.5
35.28	230	14.67	2.5420	2.5412	1.2
38.93	233	9.76	2.3115	2.3128	1
40.91	027	1.13	2.2040	2.2139	7.6
41.30	151	8.54	2.1840	2.1839	0.1
43.16	127	6.44	2.0943	2.0974	0.3
44.80	235	1.02	2.0213	2.0236	3
46.60	154	14.18	1.9475	1.9475	0.3
48.50	236	17.56	1.8752	1.8758	0.2
49.16	009	6.17	1.8517	1.8512	0.7

49.57	245	8.04	1.8372	1.8376	0.3
50.03	162	1.46	1.8216	1.8198	3.9
54.09	228	1.03	1.6942	1.6942	1
55.26	255	7.89	1.6610	1.6568	9.5
56.28	072	3.38	1.6333	1.6327	5.9
56.94	317	2.78	1.6158	1.6133	2.4
59.24	404	14.03	1.5583	1.5581	2
59.74	074	4.31	1.5466	1.5460	1
61.19	248	3.22	1.5133	1.5131	1.8
61.96	346	9.74	1.4965	1.4964	0.4
62.26	075	8.14	1.4899	1.4889	3.3
63.30	360	3.56	1.4680	1.4679	0.2
65.05	1 2 11	2.42	1.4326	1.4319	3.3
65.69	338	1.90	1.4201	1.4295	2
67.37	0 0 12	6.83	1.3888	1.3879	4
70.88	3 1 10	2.09	1.3285	1.32846	0.1
72.81	366	2.13	1.2978	1.2975	1.7
74.60	460	3.20	1.2710	1.2713	1.6
76.24	3 1 11	2.91	1.2478	1.2477	1.2
78.42	381	2.58	1.2184	1.21804	1.3
79.17	382	1.74	1.2087	1.2085	3.2
83.57	1 4 13	1.15	1.1560	1.1559	1.2
84.21	1 2 14	4.74	1.1488	1.1485	3.6
84.44	545	4.43	1.1462	1.1464	1.7
86.90	4 1 11	2.12	1.1200	1.1201	0.05
87.86	602	3.98	1.1102	1.11030	0.82

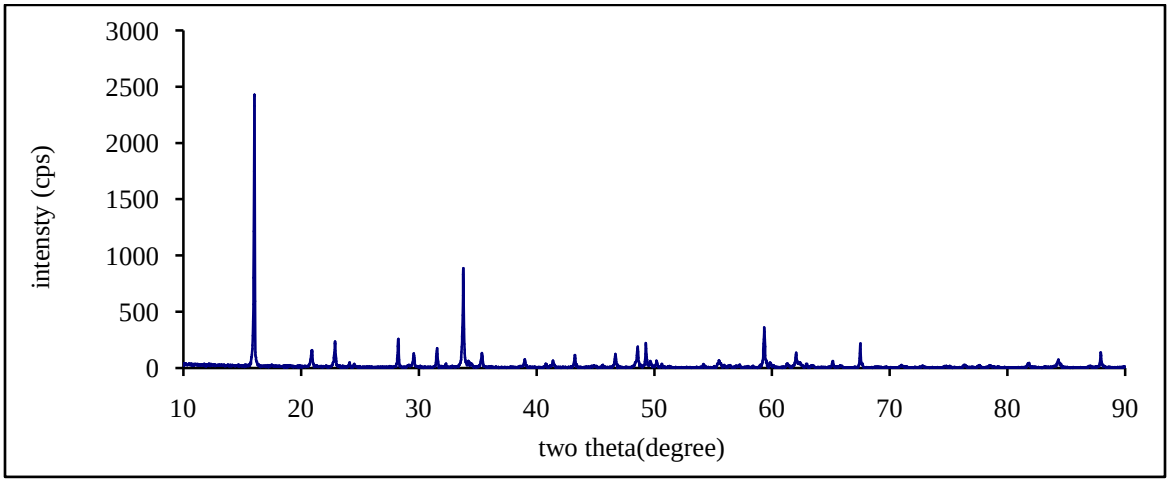

Figure 1: XRD pattern of $Na_2Zr(BO_3)_2$

FTIR spectrum of the $Na_2Zr(BO_3)_2$ compound is shown in Figure 2. Some selected IR bands of the functional groups of $Na_2Zr(BO_3)_2$ are given in Table 2. Firstly, the peak values were compared with the characteristic values of the BO_3^{-3} functional group [15]. For the planar, triangular $(BO_3)^{-3}$ group, the wavenumbers are in the region ν_3:1000-1300 cm^{-1} (asymetric stretch B-O, broad and strong), ν_1: 900-1000 cm^{-1} (symetric stretch B-O, weak), ν_2:650-800 cm^{-1} (out-of plane bend sharp and strong) and ν_4 :450-650 cm^{-1}(in-plane bend, medium). It is clearly that shown that the crystal system of $Na_2Zr(BO_3)_2$ has mainly had basic structural units of $(BO_3)^{-3}$.

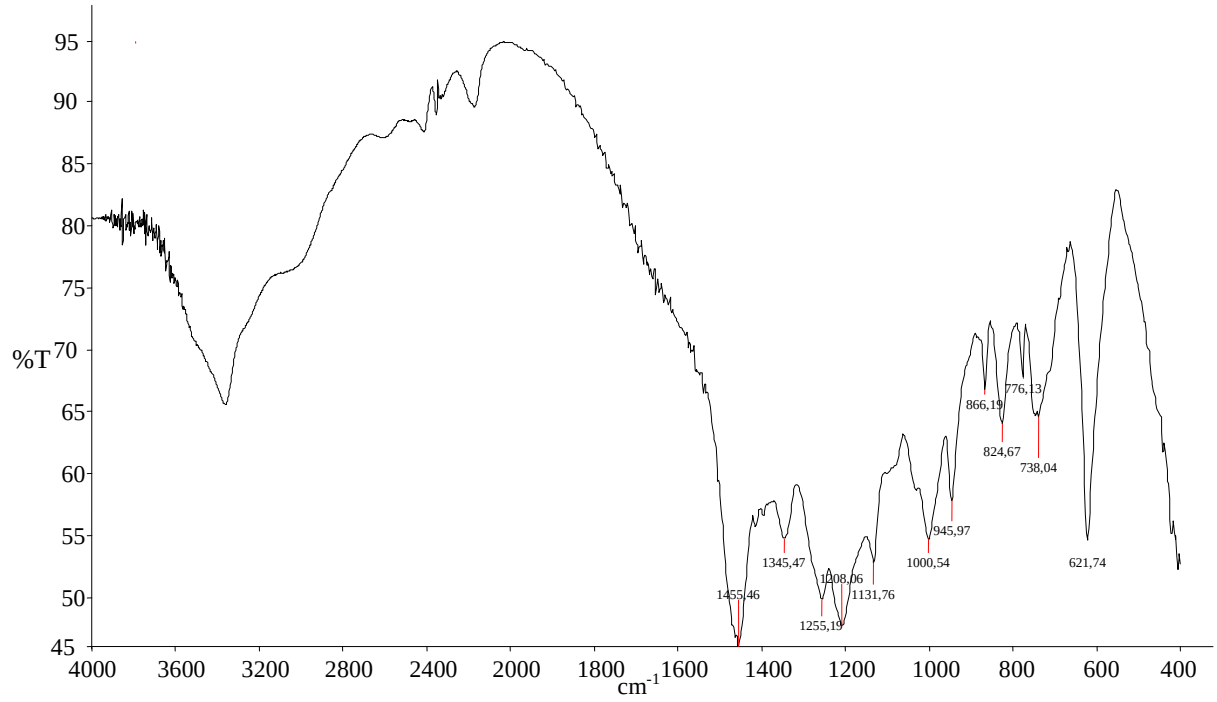

Figure 2: IR spectrum of $Na_2Zr(BO_3)_2$ in transmission mode

Figure 3a shows the temperature and excitation power density dependent PL spectra of $Na_2Zr(BO_3)_2$. For the temperature dependent measurement, the laser excitation power density was maintained at approx. 0.5 W/cm^2. The excitation power density dependent measurements were taken at 20 K. From the first seen, both spectra were dominated by one broad peaks centered at about 515 nm. However, this peak was decomposed into two peaks centered at about 512 and 567 nm with the Full Width at Half Maximum (FWHM) of 36 and 52 nm by applying Gauss fitting as shown in inset. The dependence of dominant peak (512 nm) wavelength and its FWHM obtained from best Gussian fittings on temperature and excitation power density is shown Figure 3b. As the temperature increase the peak wavelength shifts to shorter wavelength (higher energy) polynomial in a second order with much less dependent compared to first order variation. The difference between 20 and room temperature peak wavelength is found to be as about 8 nm. This temperature behavior of the peak position does not fallow the expected band gap shrinkage of the solids. On the other hand, the peak wavelength decreases almost linearly as the excitation power density increases. The difference between peak wavelength of the lowest and highest excitation power density (with about two orders of magnitude difference in power densities) is found as about 7 nm. The temperature dependence of the FWHM shows the characteristic broadening effect associated with the optical phonon scattering. At lower temperature, acoustic phonons can also be effective in lesser extent. The difference between FWHM of 20 and 300 K spectra is about 3 nm. However, it has been realized that FWHM of the main peak with a value of approx. 36 nm are almost independent from excitation power density. The variation of the integrated intensity as a function of temperature and excitation power density is shown in figure 3c. In this representation, the integrated intensities were normalized to the highest values within themselves. As seen from the figure, the total integrated intensities increase linearly with the temperature and polynomial in second order with excitation power density. As reported by Guifang Ju *et al*. the band gap of $K_2Zr(BO_3)_2$ was determined to be 5.05 eV. Therefore, the peaks observed in our sample must originate from some deep defects. Under UV light excitation, a broad persistent luminescence emission band located at ~485 nm, which was attributed to charge transfer in the zirconium complex was also reported in this

paper. From the analysis of temperature and excitation dependence of PL spectra of our $Na_2Zr(BO_3)_2$ sample and literature, these transitions at about 512 and 567 nm could be attributed to two different types of very deep defects present. The origin of these defects are unknown but could be related to oxygen deficiencies, intrinsic or extrinsic interstitial impurities.

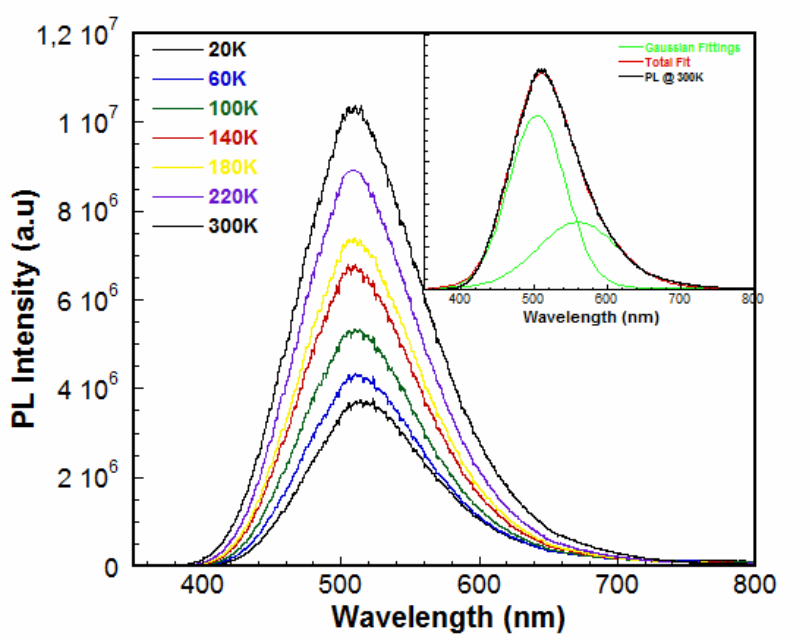

Figure 3a: The PL spectra taken at different temperature at fixed excitation power density of 0.5 W/cm^2 (a) and excitation power density at 20 K (b). The insets show the applied Gaussian fittings as examples for both measurements. The best total fit to experimental data were realized by assigning two peaks.

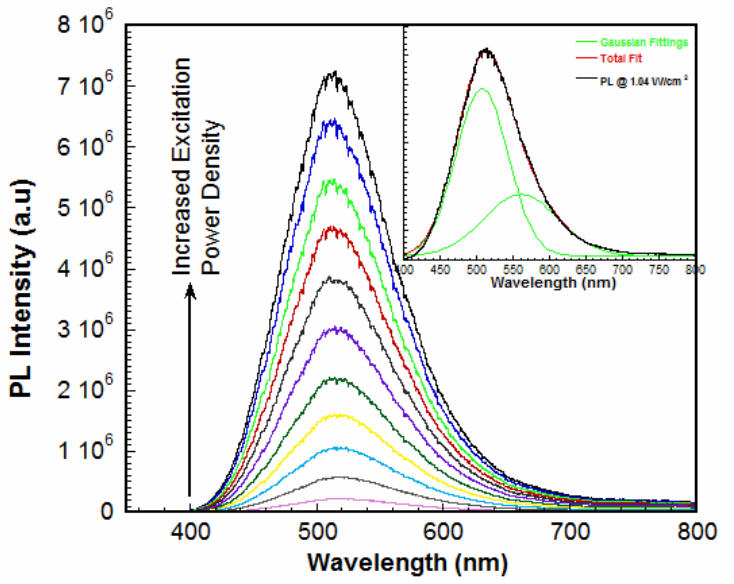

Figure 3b: The variation of the peak wavelength (having the highest intensity among two) and its FWHM as a function of both temperature and excitation power density. The solid lines show the best linear and polynomial fits discussed in the text.

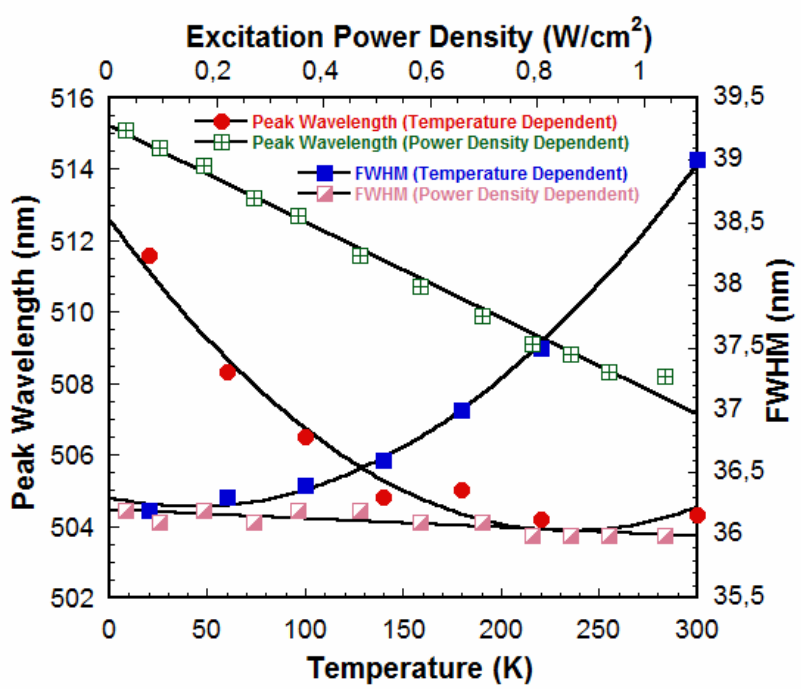

Figure 3c: The variation of normalized integrated intensity as a function of temperature and excitation power density. The solid lines show the best linear and polynomial fits discussed in the text.

Surface morphology of the $Na_2Zr(BO_3)_2$ was also investigated by scanning electron microscope. SEM measurements were performed at Quanta FEG 200. The surface morphology of $Na_2Zr(BO_3)_2$ is shown in Fig. 4 (a) and (b). As seen in the figure crystals consisting of irregular shaped particles. Small grains located on the surface of larger crystals give rise to inhomogeneous size distribution. Awarage particles size distribution estimated from the SEM images fits in the range of 10 to 50 µm.

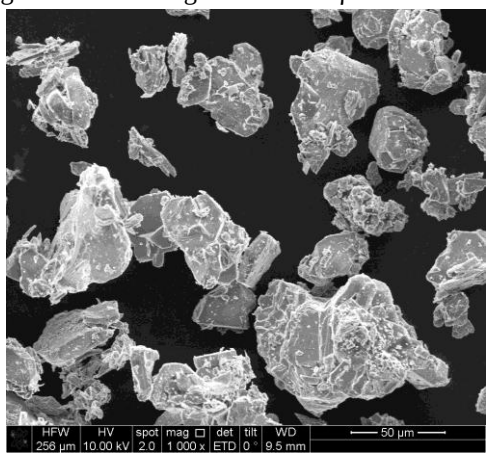

Figure 4a: SEM images of $Na_2Zr(BO_3)_2$.

Figure 4b: SEM images of $Na_2Zr(BO_3)_2$.

Conclusion

$Na_2Zr(BO_3)_2$, which is a self- luminated compound, is successfully synthesized.. The crystal structure of $Na_2Zr(BO_3)_2$ was determined by powder XRD technique. It has orthorombic crystal system with the cell parameters

of a=6.7212, b=11.6591 ve c=16.6653 Å. $Na_2Zr(BO_3)_2$ is obtained by solid state chemical reaction between the initial reactants of Na_2CO_3, ZrO_2, H_3BO_3 mixed as mol ratio of 2:1:2 in order. The optimized reaction temperature was assigned as 1000 ^oC. $Na_2Zr(BO_3)_2$ shows permanent luminescence behavior without doping with any PL activator element.

Acknowledgement
Authors acknowledge the support from Science & Technology Research and Application Center of Balikesir University.

References

1. Attfield, J. P., et al. (1999). Synthesis, structure and properties of a semivalent iron oxoborate, Fe 2OBO3. *Journal of Materials Chemistry*, 9.1: 205-209.
2. Keszler, Douglas A. (1999). Synthesis, crystal chemistry, and optical properties of metal borates. *Current Opinion in Solid State and Materials Science*, 4.2: 155-162.
3. Akella, Annapoorna, and Douglas A. Keszler. (1994). Buetschliite Derivative K2Zr (BO3) 2. *Inorganic Chemistry*, 33.7: 1554-1555.
4. He, Ling, Yuhua Wang, and Hui Gao. (2007). Characterization of the VUV excitation spectrum of BaZr (BO 3) 2: Eu. *Journal of luminescence*, 126.1: 182-186.
5. Wang, Yuhua, et al. (2004). Identification of charge transfer (CT) transition in (Gd, Y) BO 3: Eu phosphor under 100–300nm. *Journal of Solid State Chemistry*, 177.7: 2242-2248.
6. Schultze, D., K-Th Wilke, and Ch Waligora. (1971). Zur Chemie in Schmelzlösungen. IV. Darstellung von kristallinen Boraten M2+ M4+ (BO3) 2. *Zeitschrift für anorganische und allgemeine Chemie*, 380.1: 37-40.
7. Blasse, G. (1986). Energy transfer between inequivalent Eu2+ ions. *Journal of Solid State Chemistry*, 62.2: 207-211.
8. Matsuzawa, T., et al. (1996). A New Long Phosphorescent Phosphor with High Brightness, SrAl2 O 4: Eu2+, Dy3+. *Journal of the Electrochemical Society*, 143.8: 2670-2673.
9. Diaz, Anthony, and Douglas A. Keszler. (1997). Eu2+ luminescence in the borates X2Z (BO3) 2 (X= Ba, Sr; Z= Mg, Ca). *Chemistry of materials*, 9.10: 2071-2077.
10. Ju, Guifang, et al. (2017). Persistent luminescence in the self-activated K 2 Zr (BO 3) 2. *RSC Advances*, 7.7: 4190-4195.
11. Van den Eeckhout, Koen, Dirk Poelman, and Philippe F. Smet. (2013). Persistent luminescence in non-Eu2+-doped compounds: a review. *Materials*, 6.7: 2789-2818.
12. Blasse, G., E. W. J. L. Oomen, and J. Liebertz. (1986). On the luminescence of the bismuth borates BiB3O6 and Bi3B5O12. *physica status solidi, (b)* 137.1.
13. Balcerzyk, M., et al. (2000). Future hosts for fast and high light output cerium-doped scintillator. *Journal of Luminescence*, 87: 963-966.
14. Wu, E. (1989). POWD, an interactive program for powder diffraction data interpretation and indexing. *Journal of applied crystallography*, 22.5: 506-510.
15. Pan, Shilie, et al. (2006). Synthesis, structure and properties of Pb 2 CuB 2 O 6. *Materials research bulletin*, 41.5: 916-924.